

Communication: Barium ions and helium nanodroplets: Solvation and desolvation

Xiaohang Zhang and Marcel Drabbels

Laboratoire de Chimie Physique Moléculaire, Swiss Federal Institute of Technology Lausanne (EPFL), CH-1015 Lausanne, Switzerland

(Received 29 June 2012; accepted 24 July 2012; published online 3 August 2012)

The solvation of Ba^+ ions created by the photoionization of barium atoms located on the surface of helium nanodroplets has been investigated. The excitation spectra corresponding to the $6p\ ^2P_{1/2} \leftarrow 6s\ ^2S_{1/2}$ and $6p\ ^2P_{3/2} \leftarrow 6s\ ^2S_{1/2}$ transitions of Ba^+ are found to be identical to those recorded in bulk He II [H. J. Reyher, H. Bauer, C. Huber, R. Mayer, A. Schafer, and A. Winnacker, *Phys. Lett. A* **115**, 238 (1986)], indicating that the ions formed at the surface of the helium droplets become fully solvated by the helium. Time-of-flight mass spectra suggest that following the excitation of the solvated Ba^+ ions, these are being ejected from the helium droplets either as bare Ba^+ ions or as small Ba^+He_n ($n < 20$) complexes. © 2012 American Institute of Physics. [<http://dx.doi.org/10.1063/1.4743900>]

The high cooling rate, low temperature, and weak interactions of helium nanodroplets with other species render them an ideal matrix for spectroscopic characterization of atoms, molecules, and clusters.^{1,2} Notwithstanding the weak interaction between an impurity and helium, differences in interaction strength can lead to quite different solvation structures of the impurity. For example, while positive ions are located in the interior of helium droplets surrounded by a strongly compressed helium solvation shell,^{3–5} alkali and alkaline earth atoms reside on the surface of the helium droplets forming a dimple structure.^{6–9} These differences are also reflected in the absorption spectra of the impurities. The effect of the changing interaction between dopant and helium environment is best exemplified by studies on the Rydberg series of the alkali and alkaline earth atoms located on the surface of helium droplets.^{10–14} Initially, the repulsive interaction of the atom with the helium increases with principal quantum number n , resulting in increasingly blue-shifted and broadened transitions. For higher Rydberg states where the mean electron orbital radius becomes larger than the droplet radius, $n \sim 10$, the repulsive interaction between the electron and the helium decreases and the attractive interaction between the ionic core and the helium becomes more important. This interaction change is reflected in the excitation spectra by narrow and red-shifted transitions. As the principle quantum number increases further, the mean electron orbit radius becomes so large that the system resembles an ion-containing helium droplet. Although these exotic states have been observed, the experiments did not provide information on the location of the ionic core.¹¹ As a matter of fact, other experiments in which surface located atoms are photoionized neither provide direct information on the location of the created ion, as the time-of-flight mass spectra only indicate that the created ions remain attached to the helium droplets.¹⁵ The intriguing question whether ions that are created at the surface of the droplets, become solvated by the helium as might be expected based on the energetics of the system or remain at the surface due to the existence of a small energy barrier abides to be resolved.

The dynamics following the photoionization of neutral species in or on helium nanodroplets are closely related to the dynamical processes induced by the excitation of ions in helium droplets. It was recently found that upon vibrational excitation of molecular ions, these ions desolvate from the helium nanodroplets by a non-thermal process in which they are ejected from the droplets.^{16–18} This is in stark contrast with the thermal evaporation process found for neutral dopants.^{19,20} The experiments indicate that the desolvation is initiated by the vibrational excitation of the ionic impurity. However, it is not straightforward to determine whether electronic excitation can also initiate these processes since electronic excitation in molecular ions is readily converted to vibrational energy by radiative and non-radiative relaxation processes.¹⁷ Hence, to answer this question an atomic ionic probe is preferred.

In this communication, we address the two issues raised above, i.e., possible solvation of surface generated ions and the desolvation of excited atomic ions, using barium as probe. Following the photoionization of barium atoms located on the surface of helium droplets, excitation spectra are recorded corresponding to the $6p\ ^2P_{1/2} \leftarrow 6s\ ^2S_{1/2}$ and $6p\ ^2P_{3/2} \leftarrow 6s\ ^2S_{1/2}$ transitions of Ba^+ . By comparing these spectra to those recorded of Ba^+ in bulk He II,²¹ solvation of the ions by the helium can be established. Insight into the desolvation of the excited barium ions is then obtained from time-of-flight mass spectra and the speed distributions of the desolvated ions. Here, we report on the first results obtained on this system, a more detailed study will be published later.

Details of the experimental setup have been reported in previous publications.^{22,23} Helium droplets are formed by expanding high-purity ^4He gas at stagnation pressure of 30 bars into vacuum through a cryogenically cooled $5\ \mu\text{m}$ orifice. The helium droplets pick up barium atoms as they pass through an oven containing barium dendritic crust. The temperature of the oven is adjusted to ensure that the helium droplets contain on average less than one Ba atom. Via a differential pumping stage the doped droplets enter a velocity map imaging

setup that can also be used for time-of-flight measurements. At the center of the imaging setup the droplet beam is crossed at right angles by two counter-propagating laser beams. The barium-doped helium droplets are ionized by one-photon absorption of UV radiation provided by a frequency-doubled dye laser operated at a repetition rate of 20 Hz. The UV light which has a pulse energy of 0.3 mJ is weakly focused onto the droplet beam by a 40 cm focal length lens. After a time delay of typically 185 ns, the barium ions are excited via the $6p \leftarrow 6s$ transition by visible radiation in the wavelength range of 430–500 nm provided by another Nd:YAG pumped dye laser. The intensity of the laser beam, which has a diameter of approximately 1.5 mm, is adjusted using a combination of a half-wave plate and a linear polarizer. The ions created by the lasers are accelerated by the electric fields of the imaging setup and projected onto a position sensitive detector consisting of a set of microchannel plates (MCP) and a phosphor screen. A high-resolution CCD camera takes snapshots of the phosphor screen at each laser shot and the individual images are analyzed online. By gating the MCP detector, mass specific excitation spectra can be recorded by monitoring the number of ion impacts as a function of laser frequency. By feeding the electrical signal from the phosphor screen into a multichannel scaler time-of-flight measurements can be performed.

In the present experiment, barium atoms located on the surface of the droplets are excited just above the ionization threshold by the absorption of a $42\,283\text{ cm}^{-1}$ photon.¹⁰ The ions created at the droplet surface can either directly desorb from the droplets, remain located at the surface or become solvated by the helium. In the case of immediate desorption, excitation of the bare Ba^+ ion via the $6p \leftarrow 6s$ transitions will not lead to a detectable ion signal. In case the barium ion remains located at the surface of the droplet, it can be expected, based on the analogy with surface located alkali atoms, that excitation of the Ba^+ ion leads to its desorption from the surface.^{7,12,24} If the Ba^+ ion becomes solvated by the helium, excitation might lead to its ejection from the helium matrix, analogous to what has been found for molecular ions.^{16,18} In the latter two scenarios, excitation of the ions can be readily detected, as this will lead to a depletion of the number of ion-containing helium droplets and the appearance of bare Ba^+ or small Ba^+He_n complexes. The spectra corresponding to surface located and solvated Ba^+ will be quite dissimilar due to the difference of the surrounding environment. In the lower panel of Fig. 1 we report the $6p \leftarrow 6s$ excitation spectrum recorded by monitoring the yield of Ba^+ as function of excitation frequency following the ionization of barium atoms located at the surface of helium droplets consisting on average of 2700 atoms. Similar spectra have been obtained for different droplet sizes and time delays between the laser pulses. The spectrum is characterized by some sharp lines and several broad features. Most of the spectral features, indicated by an asterisk, can be attributed to transitions involving neutral barium atoms. A detailed discussion of these features is beyond the scope of this communication and will be provided in a forthcoming publication. The two main resonances located at $20\,750\text{ cm}^{-1}$ and $22\,500\text{ cm}^{-1}$ can be attributed to the $6p\ ^2P_{1/2} \leftarrow 6s\ ^2S_{1/2}$ (D1) and $6p\ ^2P_{3/2} \leftarrow 6s\ ^2S_{1/2}$ (D2) transitions, respectively.

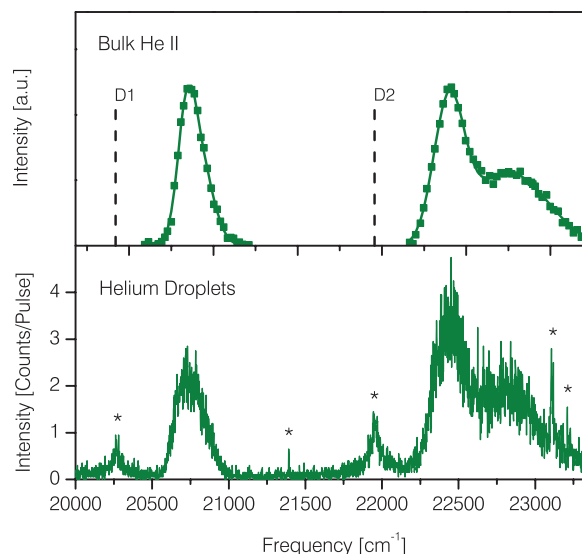


FIG. 1. Upper panel: Excitation spectrum corresponding to the $6p \leftarrow 6s$ transition of Ba^+ in bulk He II (adapted from Ref. 21). The gas phase transitions are indicated by the vertical dotted lines.²⁵ Lower panel: The same transition recorded following the ionization of barium atoms located on the surface of helium nanodroplets consisting on average of 2700 atoms. The spectral features labeled with asterisk are transitions related to neutral Ba.

Whereas the D1 transition appears as a single slightly asymmetric line, the D2 transition has a pronounced shoulder and appears to consist of two contributions. The broadening of these transitions and their shifts with respect to the gas phase can be attributed to the repulsive interaction between the excited ion having the $6p$ orbital protruding into the electrophobic He environment.²⁵ The splitting of the D2 transitions is also observed in the Cs atom,²⁶ which has the same electron configuration as Ba^+ . It can be thought of in terms of the two $\text{Ba}^+\text{-He}$ pair potentials, $^2\Sigma_{1/2}$ and $^2\Pi_{3/2}$, correlating to the $6p\ ^2P_{3/2}$ state of the free barium ion.^{27,28} In the upper panel of Fig. 1 the fluorescence excitation spectrum of Ba^+ recorded in bulk He II is presented.²¹ A careful comparison of the two spectra reveals that the resonances are identical, having exactly the same positions and widths. The relative intensities of the two transitions are also very similar in both spectra, even though these spectra have been recorded using different observables, i.e., fluorescence vs. ion desolvation. The excellent agreement of the spectra with those recorded in bulk He II strongly suggests that the barium ions reside in the interior of the helium droplets. This conclusion is reinforced by considering the corresponding transition of Cs which reveals a large spectral difference between solvated and surface bound atoms.²⁶ The spectra thus provide clear evidence that after their creation at the surface of the droplets, the Ba^+ ions become fully solvated by the helium on the 100 ns timescale of the experiment.

To gain insight into the desolvation mechanism of the excited Ba^+ ions, the Ba^+ signal has been recorded as function of laser intensity. In Fig. 2 the data are presented for excitation of Ba^+ via the D2 transition at $22\,425\text{ cm}^{-1}$ for droplets consisting on average of 6000 helium atoms. The data show the typical $[1 - \exp(-\sigma I)]$ dependence on the laser intensity I for a one-photon excitation process having an

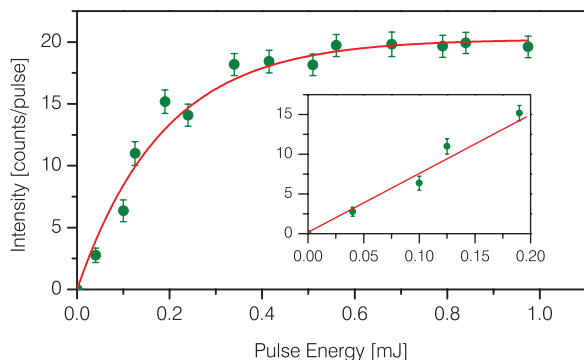


FIG. 2. Laser intensity dependence of the Ba^+ ion signal when exciting the D2 transition at $24\,425\text{ cm}^{-1}$ (dots). The line is a fit to the expression for single absorption, see text for details. Inset: close up of the initial increase of the ion signal with laser intensity.

absorption cross section σ . The inset of Fig. 2 shows linear intensity dependence of the ion signal for low laser intensity, underlining the single-photon character of the process. It should be mentioned that the same dependence is found for the D1 transition. A fit to the data, indicated by the solid line, yields an integrated absorption cross section of $\sim 2 \times 10^{-14}\text{ cm}$, a value comparable with that of the free ion.²⁹ These observations imply that the absorption of a single photon leads to the desolvation of the barium ion.

Additional information on the desolvation process can be obtained by mass spectrometry. Time-of-flight mass spectra have been recorded following ionization of barium atoms located on the surface of helium droplets consisting on average of 6000 atoms using a photon energy of $42\,283\text{ cm}^{-1}$. At this photon energy a large background signal is observed in the time-of-flight spectra at the mass of the helium droplets. This background contribution has been subtracted from the mass spectra reported in the upper panel of Fig. 3, which explains their rather limited signal-to-noise ratio. The initial Ba^+ -containing helium droplet size distribution, presented by the grey trace, is rather well described by a log-normal distribution corresponding to a mean droplet size of 5750 helium atoms, which compares well to the expected value of 6000 based on the expansion conditions. The time-of-flight mass spectrum recorded in the presence of $20\,713\text{ cm}^{-1}$ radiation, corresponding to the absorption maximum of the D1 transition, is presented by the green trace. Comparison of the two spectra reveals a significant depletion of the signal level in the 12 000–40 000 amu mass range, corresponding to Ba^+ containing helium droplets consisting of 3000–10 000 helium atoms. This reduction is accompanied with a remarkable signal increase in the low mass range. As can be seen in the lower panel of Fig. 3, excitation of the embedded barium ions not only yields bare Ba^+ but also small $\text{Ba}^+\text{-He}_n$ complexes with up to 20 helium atoms. Similar results are obtained for excitation of the barium ion via the D2 transition.

In order to firmly establish the desolvation mechanism, knowledge about the quantum state of the detected barium ions is required. Unfortunately, the experiment does not provide this information. However, there are several reasons to assume that the detected ions are 6p excited Ba^+ . The first indication is provided by the experiment performed in bulk He

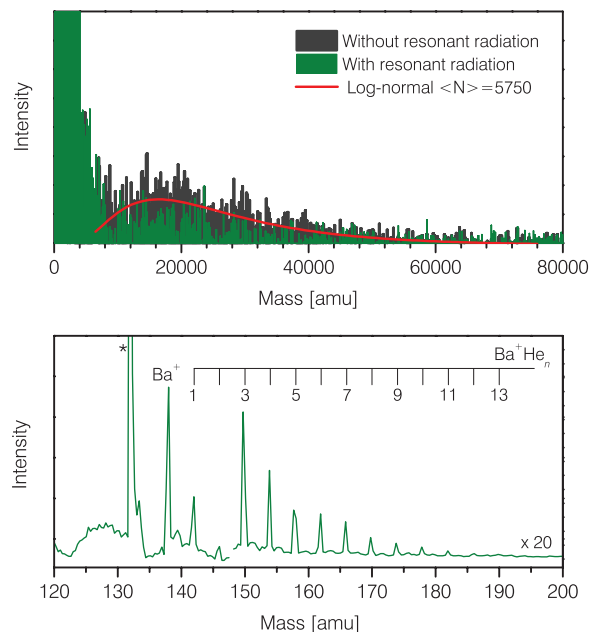


FIG. 3. Time-of-flight mass spectra following the photoionization of barium atoms attached to helium nanodroplets. Upper panel: The initial high mass distribution (grey trace) with fitted log-normal distribution (red line) and mass distribution in the presence of $20\,713\text{ cm}^{-1}$ radiation resonant with the D1 transition (green trace). Lower panel: Mass spectrum in the low mass range resulting from the excitation of the barium ion. The line denoted by an asterisk corresponds to Ba^+ ions resulting from the ionization process.

II.²¹ The observed dispersed fluorescence spectra indicate that the system has relaxed to an optimized helium configuration for the 6p excited Ba^+ ion before photon emission. This suggests that direct non-radiative relaxation to the ground state is not very likely on the time scale of the experiment. Another indication is provided by considering the properties of Cs which has the same electron configuration as Ba^+ and a very similar excited state interaction with helium.^{27,30} Experiments in bulk He II indicate that Cs relaxes purely radiatively.³⁰ If it is assumed that the excited Ba^+ relaxes exclusively by radiation, the maximum amount of energy released into the droplets amounts to 1700 cm^{-1} .²¹ If one assumes that the metastable $5d\ ^2D_{3/2}$ state populated by emission from the excited 6p state, relaxes non-radiatively to the ground state on the time scale of the experiment a total of $\sim 5500\text{ cm}^{-1}$ would be deposited into the droplets. Taking the binding energy of a helium atom to the droplet to be 5 cm^{-1} , the energy release would lead to the evaporation of ~ 350 or ~ 1100 helium atoms, depending on the relaxation pathway.³¹ The evaporation of helium atoms would be observed in the time-of-flight spectrum as a shift of the mass distribution towards lower masses. However, the time-of-flight spectra indicate an overall signal reduction in the 12 000–40 000 amu mass range, which is clearly incompatible with the evaporation model. The time-of-flight spectra rather point to a desolvation mechanism in which the barium ions are ejected from the helium droplets, analogous to what has been proposed for molecular ions.^{16,18} We would like to point out that even if non-radiative relaxation to the ground state would occur, and thus the full photon energy would be released into the droplet, a thermally

driven evaporation process would not be able to fully account for the observed depletion in the high mass range.

The velocity distribution of the desolvated barium ions provides additional insight into dynamical evolution of the system. Details of these distributions will be reported in the future; here we would just like to mention that they can be accurately described by a Maxwell-Boltzmann distribution corresponding to a translational temperature of approximately 180 K. This temperature is almost an order of magnitude larger than that observed for neutral systems that are known to cool by evaporation.³² The speed distributions thus also seem to point to a desolvation mechanism in which the excited Ba⁺ ions are ejected from the droplets instead of an evaporative cooling mechanism.

In summary, we have recorded excitation spectra corresponding to the $6^2P_{1/2} \leftarrow 6^2S_{1/2}$ and $6^2P_{3/2} \leftarrow 6^2S_{1/2}$ transitions for Ba⁺ ions created by the photoionization of barium atoms located at the surface of helium nanodroplets. Comparison of the spectra with those recorded of Ba⁺ ions in bulk He II indicates that the barium ions that are initially located at the surface of helium nanodroplets are fully solvated by the helium. In addition, time-of-flight mass spectra indicate that following the excitation of the solvated ions, these are ejected from the helium droplets as Ba⁺ ions or small Ba⁺He_n ionic complexes.

We gratefully acknowledge the financial support provided by the Swiss National Science Foundation (Grant No. 200020_129623) and thank Mr. Nils Brauer for stimulating discussions.

- ¹J. P. Toennies and A. F. Vilesov, *Angew. Chem., Int. Ed.* **43**, 2622 (2004).
²M. Y. Choi, G. E. Douberly, T. M. Falconer, W. K. Lewis, C. M. Lindsay, J. M. Merritt, P. L. Stiles, and R. E. Miller, *Int. Rev. Phys. Chem.* **25**, 15 (2006).
³A. Nakayama and K. Yamashita, *J. Chem. Phys.* **112**, 10966 (2000).
⁴C. C. Duminuco, D. E. Galli, and L. Reatto, *Physica B* **284**, 109 (2000).
⁵K. K. Lehmann and J. A. Northby, *Mol. Phys.* **97**, 639 (1999).
⁶F. Ancilotto, E. Cheng, M. W. Cole, and F. Toigo, *Z. Phys. B: Condens. Matter* **98**, 323 (1995).

- ⁷F. Stienkemeier, J. Higgins, C. Callegari, S. I. Kanorsky, W. E. Ernst, and G. Scoles, *Z. Phys. D: At., Mol. Clusters* **38**, 253 (1996).
⁸A. Hernando, R. Mayol, M. Pi, M. Barranco, F. Ancilotto, O. Bunermann, and F. Stienkemeier, *J. Phys. Chem. A* **111**, 7303 (2007).
⁹F. Stienkemeier, F. Meier, and H. O. Lutz, *J. Chem. Phys.* **107**, 10816 (1997).
¹⁰E. Loginov and M. Drabbels, *J. Chem. Phys.* **136**, 154302 (2012).
¹¹E. Loginov and M. Drabbels, *Phys. Rev. Lett.* **106**, 083401 (2011).
¹²E. Loginov, C. Callegari, F. Ancilotto, and M. Drabbels, *J. Phys. Chem. A* **115**, 6779 (2011).
¹³F. Lackner, G. Krois, M. Koch, and W. E. Ernst, *J. Phys. Chem. Lett.* **3**, 1404 (2012).
¹⁴F. Lackner, G. Krois, M. Theisen, M. Koch, and W. E. Ernst, *Phys. Chem. Chem. Phys.* **13**, 18781 (2011).
¹⁵M. Theisen, F. Lackner, and W. E. Ernst, *Phys. Chem. Chem. Phys.* **12**, 14861 (2010).
¹⁶S. Smolarek, N. B. Brauer, W. J. Buma, and M. Drabbels, *J. Am. Chem. Soc.* **132**, 14086 (2010).
¹⁷N. B. Brauer, S. Smolarek, X. H. Zhang, W. J. Buma, and M. Drabbels, *J. Phys. Chem. Lett.* **2**, 1563 (2011).
¹⁸X. Zhang, N. B. Brauer, G. Berden, A. M. Rijs, and M. Drabbels, *J. Chem. Phys.* **136**, 044305 (2012).
¹⁹D. M. Brink and S. Stringari, *Z. Phys. D: At., Mol. Clusters* **15**, 257 (1990).
²⁰J. M. Merritt, G. E. Douberly, and R. E. Miller, *J. Chem. Phys.* **121**, 1309 (2004).
²¹H. J. Reyher, H. Bauer, C. Huber, R. Mayer, A. Schafer, and A. Winnacker, *Phys. Lett. A* **115**, 238 (1986).
²²A. Braun and M. Drabbels, *J. Chem. Phys.* **127**, 114303 (2007).
²³E. Loginov and M. Drabbels, *J. Phys. Chem. A* **111**, 7504 (2007).
²⁴A. Hernando, M. Barranco, M. Pi, E. Loginov, M. Langlet, and M. Drabbels, *Phys. Chem. Chem. Phys.* **14**, 3996 (2012).
²⁵Y. Ralchenko, A. Kramida, J. Reader, and NIST ASD Team, NIST Atomic Spectra Database, version 4.1, 2011.
²⁶O. Bunermann, M. Mudrich, M. Weidemuller, and F. Stienkemeier, *J. Chem. Phys.* **121**, 8880 (2004).
²⁷Y. Fukuyama, Y. Moriwaki, and Y. Matsuo, *Phys. Rev. A* **69**, 042505 (2004).
²⁸O. Bunermann, G. Droppelmann, A. Hernando, R. Mayol, and F. Stienkemeier, *J. Phys. Chem. A* **111**, 12684 (2007).
²⁹J. E. Sansonetti and W. C. Martin, *J. Phys. Chem. Ref. Data* **34**, 1559 (2005).
³⁰T. Kinoshita, K. Fukuda, T. Matsuura, and T. Yabuzaki, *Phys. Rev. A* **53**, 4054 (1996).
³¹F. Dalfovo, A. Latri, L. Pricaupenko, S. Stringari, and J. Treiner, *Phys. Rev. B* **52**, 1193 (1995).
³²A. Braun and M. Drabbels, *J. Chem. Phys.* **127**, 114305 (2007).